

549-90

309529

N91-14149

P-3

interstellar medium (ISM)

## IMAGING SPECTROPHOTOMETRY OF THE NUCLEAR OUTFLOW OF NGC 1068

Gerald Cecil, *Institute for Advanced Study*, Princeton NJ 08540

charge coupled devices (CCD)

This observational program (in conjunction with R. B. Tully [*IfA*, Honolulu], and J. Bland [*Rice U.*, Houston]) aims to constrain the kinematic organization and dominant excitation mechanisms of ionized gas in active galaxies. More generally, we are interested in the dynamics of radiative, supersonic flows in the ISM. Imaging Fabry-Perot interferometers and low-noise CCDs are used for complete spatial coverage of the complex gas distribution in circumnuclear narrow-line regions (NLRs). Extranuclear emission line widths in NLRs can exceed  $3000 \text{ km s}^{-1}$ , so to avoid inter-order confusion we use an etalon of  $4000 \text{ km s}^{-1}$  free spectral range to map [N II]  $\lambda\lambda 6548, 6583$  and H $\alpha$ . To maximize spatial resolution, we select nearby active systems independent of luminosity but known to possess interesting morphologies and/or high-velocity extranuclear ionized gas. Monochromatic images (FWHM  $\sim 65 \text{ km s}^{-1}$ ) have thus far been obtained in  $1''$  or better seeing at the U. Hawaii 2.2m, CFH 3.6m, and CTIO 4.0m telescopes. These are stacked into grids of line profiles, of spectrophotometric quality, at sub-arcsecond increments across a  $3'$  field. To handle the  $\sim 20,000 - 300,000$  useful spectra that arise from a typical night's work, we have developed a complete analysis and reduction package for VAX and Sun image workstations. Reduction involves parametrization of  $\sim 10^8$  raw data points to a few maps (e.g. velocities of each kinematic subsystem, continuum-free line fluxes) containing  $\sim 10^5$  pixels. We identify kinematic and structural symmetries by examining these maps and the point to point variations of the synthesized line profiles. The combination of monochromatic images and full spatial sampling of line profiles has allowed us to isolate such symmetries and has led to reliable kinematic deprojections.

The spatially extended NLR ( $\sim 6''$  radius) of NGC 1068 was mapped in N<sup>+</sup> with high spatial resolution ( $0.''8$  FWHM) at  $f/8.6$  on the U. Hawaii 2.2m telescope. After subtracting the stellar continuum at each point, I summed the monochromatic images to generate a view equivalent to that obtained with traditional narrow-band interference filters. The NLR aligns with the jet axis, but correspondence to the radio structure is vague. The stacked images synthesize emission line profiles at sub-arcsecond spatial and  $\sim 140 \text{ km s}^{-1}$  velocity resolution. Regularities in our spectra allow decomposition of the profiles into discrete kinematic subsystems. These were noted by other observers in slit spectra, but flux distributions and kinematics can now be tracked across the entire NLR and show obvious connections with the radio structure (Fig. 1). Our complete coverage allows detailed study of possible interactions of the prominent collimated radio "jet" and associated wind with the warm ionized component of the ambient ISM.

I find three major *dynamically distinct* kinematic subsystems in this NLR:

- 75% of the total dereddened NLR [N II] flux ( $\sim 12,000 [10^5 \text{ cm}^{-3} / n_e] M_\odot$ ) is contained in high-velocity gas (Fig. 1a), with approximately equal mass distributed a) to the NE, as a pair of components whose centroids are displaced symmetrically about systemic velocity by  $\pm 500 \text{ km s}^{-1}$ , with FWHMs  $\sim 750 \text{ km s}^{-1}$ ; and, b) everywhere else within  $4''$  radius, as a broad component with FWHM  $\sim 1200 \text{ km s}^{-1}$ . Double-peaked line profiles and rapid intensity gradients are found when the jet decollimates at hotspots NE and SW of the nucleus. The deprojected emission distribution shows that the radio jet is enveloped by a thick (FWHM  $\sim 3.''3 = 230 \text{ pc}$ ), center-darkened, cylinder of line emission (Fig. 2). The most intense gas emission is concentrated in a thick, conical shell with Gaussian centroid and dispersion  $1/4$  of the cylinder radius ( $\approx 5'' = 370 \text{ pc}$ ). The cone has opening angle  $85^\circ$  and axial inclination  $80^\circ$  to the line of sight (so its axis is inclined  $\sim 40^\circ$  above the disk plane in the NE quadrant); the jet axis lies closer to the disk plane. Intrinsic gas velocities approach  $2000 \text{ km s}^{-1}$  w.r.t. systemic; have form  $r^{0.6}$  with  $r$  the cylindrical radius from the jet axis; and so are inconsistent with a

7/16/93

constant velocity conical outflow. The emitting filaments are optically thick (because [O III] and [N II] profiles are similar out to radii of several arcseconds), with internal extinction. The surprisingly good agreement between modeled and observed profiles shows that profile structure is here primarily driven by geometry. Because no line broadening is incorporated or required in the model, the large extranuclear line widths in this NLR arise exclusively from geometric projection and spatial averaging of an asymmetric, large-scale flow, with *no evidence for intrinsic "turbulence" in the outflowing material*. If the filaments are confined by a directed, outflowing thermal galactic wind, their masses are  $\geq 10^{-2} M_{\odot}$ , showing that they are not BLR clouds blown to observable radii. Instead it appears that molecular cloud cores with average densities of  $\sim 10^3 \text{ cm}^{-3}$  (as derived from CO interferometry) are forced by the stellar bar (prominent in near-IR images) from radii  $\sim 20''$  into the inner NLR. There they are exposed to the wind, and the resulting surface instabilities strip their envelopes. The envelope fragments are crushed to densities of  $\sim 10^5 \text{ cm}^{-3}$  during wind acceleration, until each fragment attains pressure equilibrium with the shocked wind. The fragments are stable to thermal evaporation in the hot confining medium for the masses and velocities derived from our observations.

- Gas near systemic velocity is concentrated in the kinematic "flare" which coincides with the NE radio lobe (Fig. 1b); is edge-brightened, particularly along the NW edge of the lobe (leading w.r.t. galactic rotation); accounts for 8% of the total NLR [N II] flux ( $\sim 1.2 \times 10^5 [10^3 \text{ cm}^{-3} / n_e] M_{\odot}$ ), but negligible kinetic energy; and is also apparent in H $\alpha$  images, so is a mass enhancement. In projection this component is contiguous with high-velocity gas in the NE radio lobe, yet the only kinematic deviation from the bar-forced flow field defined by gas in the large-scale disk is localized in an expanding "ripple" around the base of the NE cone (Fig. 1d), with kinetic energy  $\sim 10^{51}$  ergs, which appears to be a stand-off shock between massive, inflowing molecular clouds and their wind-accelerated fragments.
- 9% of the total NLR [N II] flux ( $\sim 1000 [10^5 \text{ cm}^{-3} / n_e] M_{\odot}$ ) is emitted by a component which dominates within  $1''$  of the nucleus, and extends to  $2''$  radius along  $\sim 110^{\circ}$  P.A. (Fig. 1c). Its centroid is blue-shifted by  $\sim 250 \text{ km s}^{-1}$  from systemic, and has line width  $\sim 600 \text{ km s}^{-1}$  (i.e. typical of a Seyfert 2 galaxy). In the absence of a wind/ISM interaction we argue that this component would be the only manifestation of the active nucleus. Our highest-resolution images show a tight correlation of the brightest line emission with the nuclear triple radio-source ( $\sim 0.''7$  extent), in agreement with speckle line-imaging.

In summary, the combination of monochromatic images and full spatial sampling of line profiles allows kinematic decomposition of this NLR into dynamically distinct subsystems, and mapping of the flux and velocity distributions of each component. The global kinematic structure of the high-velocity outflow shows well defined, large scale symmetry. Deprojection increases kinetic energies ten-fold to  $\sim 2 \times 10^{53}$  ergs, and outflow velocities to  $1900 \text{ km s}^{-1}$ . The appearance of this NLR changes dramatically as the velocity resolution improves from the  $1000 \text{ km s}^{-1}$  ( $25 \text{ \AA}$ ) passbands traditionally employed in interference imaging to the  $65 \text{ km s}^{-1}$  resolution attained with our current etalon. Sharply defined, bright features exhibit sharp *kinematic* boundaries, and thus resemble not static, photoionized nebulae, but rather the shocked termini of hydrodynamic flows. These patterns indicate that, *down to the smallest observed scales*, the spatial morphology, kinematics, and bulk of the (kinetic and turbulent) energy of the near-nuclear ionized gas are apparently driven by the thermalization of a directed nuclear outflow along well-defined shock fronts in the ambient ISM. Relativistic electrons trace only a small fraction of the outflow. By its spatial extension the NLR of NGC 1068 provides a unique opportunity to study the dynamics of a supersonic flow in an active nucleus. *HST* will soon image NLRs in great detail, but only with second generation instrumentation will it be possible to produce kinematic maps.

We thank J. Ulvestad for the radio map and H. Thronson for the *K*-band image. This phase of our research was supported by grants NSF 86-15974 (Hawaii) and NAS8-32902 (IAS).

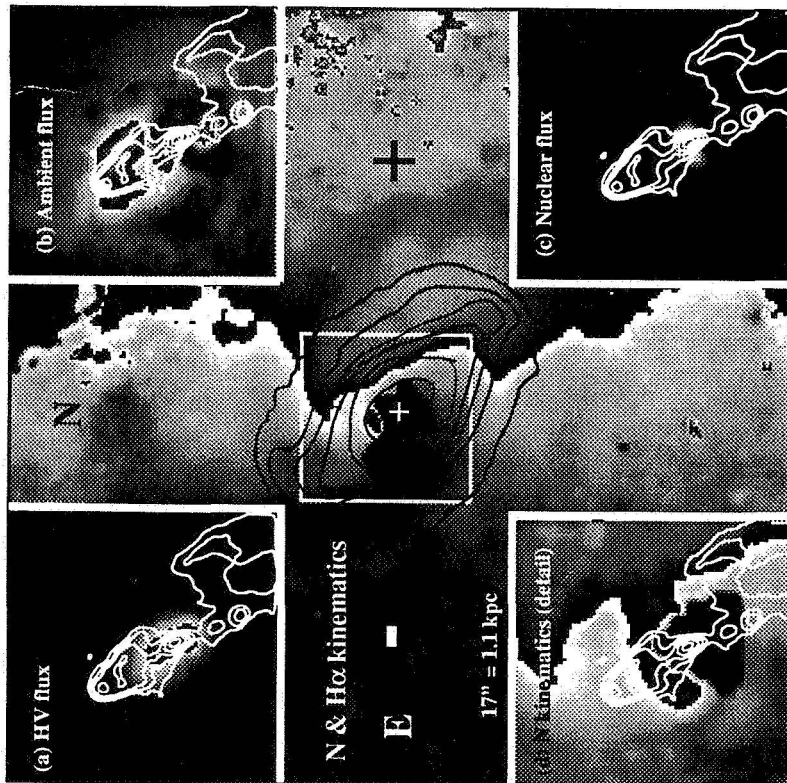


**Fig. 1 Kinematic Subsystems in the NLR of NGC 1068**

(Main figure) The large-scale disk kinematics in [N II] and H $\alpha$ . A total velocity range of  $\pm 160 \text{ km s}^{-1}$  is spanned by 2 cycles of the greyscale, which wraps near systemic velocity. We find a (KMA, disk inclination) of  $(85, 35)^\circ$  respectively, E approaching. The  $2.2\mu\text{m}$  continuum image of the stellar bar is contoured on top. The Z-shape in the center is characteristic of a bar-forced gaseous disk; the boxed region is enlarged in inserts (a-d) which plot distributions of flux (a-c) and velocity centroid (d).

(a: upper left) High-velocity gas accounts for most of the NLR mass and kinetic energy, with  $\sim 75\%$  tightly aligned with the linear part of the radio jet. Symmetries in the NLR profiles and monochromatic images suggest conical expansion of gas about the jet, with deprojected velocities  $\sim 1900 \text{ km s}^{-1}$ . 6cm continuum contours are overlaid.

(b: upper right) Ambient ISM interacting with the expanding radio lobes. Material is found: a) NE of the nucleus in a narrow velocity ( $< 60 \text{ km s}^{-1}$  FWHM) feature; and b) in an optical hotspot with somewhat broader lines, at the southern end of the linear part of the radio jet. In detail, both features are edge brightened along the leading side w.r.t. galactic rotation.

(c: lower right) The nuclear component has FWHM  $\sim 600 \text{ km s}^{-1}$  and extends along  $100^\circ$  P.A.

(d: lower left) Kinematic response of the gaseous disk to the nuclear outflow. The "ripple" across the base of the NE radio lobe ( $80 \text{ km s}^{-1}$  difference) is the only deviation from the large-scale, bar forced flow.

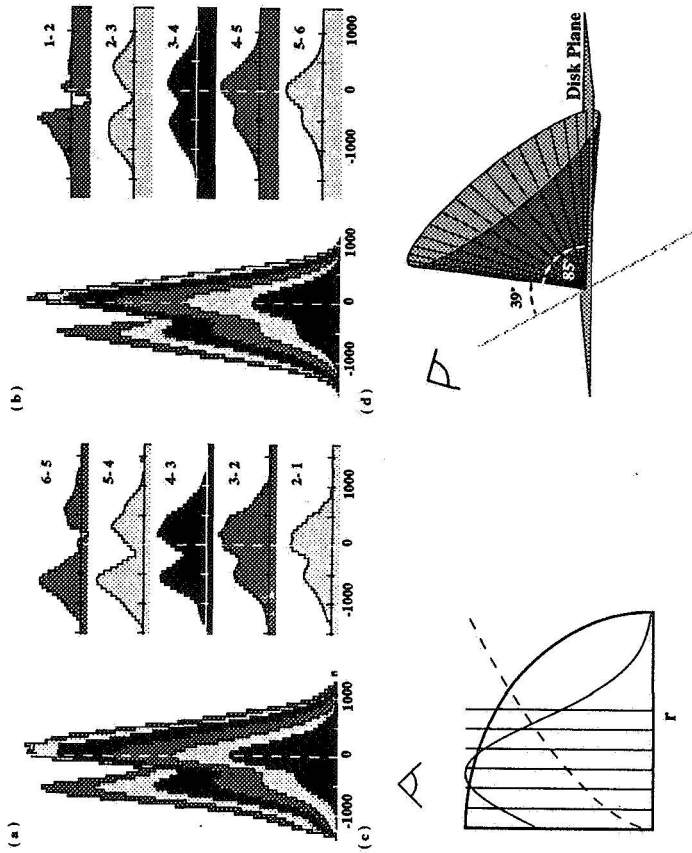


**Fig. 2 Geometry of NGC 1068 Outflow**

(a) Observed profile swath across the base of the NE radio lobe, averaged in a  $(1.0, 0.5)''$  box (along, across) the jet. Velocities relative to systemic. This profile structure constrains the outflow geometry.

(b) Model profile swath from a cylindrically expanding flow, with velocity dependence  $r_{0.6}^{0.6}$  and Gaussian emissivity centroid and dispersion 20% of the cylinder radius  $r$ ; smoothed to the velocity resolution ( $\sim 140 \text{ km s}^{-1}$  FWHM) and spatial sampling ( $0.48''$ ) of the data. The emitting clouds are assumed to be optically thick, and to absorb 60% of the incident nuclear ionizing flux.

(c) A slice through the outflowing cone, showing sample points (vertical bins) and the radial dependence of gas (emissivity, velocity) with (solid, dashed) lines. Note that emission drops on the jet axis.

(d) Schematic of inferred NLR geometry. Plane (c) intersects the cone parallel to the line of sight. The cone extends  $\sim 6''$  NE of the nucleus.